

1

2

3

4

5 Polyamine biosynthesis in *Xenopus laevis*: the gene xIAZIN2/xIODC2 encodes a lysine
6 decarboxylase

7

8

9 Ana Lambertos^{1,2} and Rafael Peñafiel^{1,2*}

10

11

12 ¹ Department of Biochemistry and Molecular Biology B and Immunology, Faculty of
13 Medicine, University of Murcia, Murcia, Spain;

14 ² Biomedical Research Institute of Murcia (IMIB), Murcia, Spain

15

16

17 *Correspondence: rapegar@um.es (RP)

18

19 **Abstract**

20 Ornithine decarboxylase (ODC) is a key enzyme in the biosynthesis of polyamines, organic
21 cations that are implicated in many cellular processes. The enzyme is regulated at the post-
22 translational level by an unusual system that includes antizymes (AZs) and antizyme inhibitors
23 (AZINs). Most studies on this complex regulatory mechanism have been focused on human
24 and rodent cells, showing that AZINs (AZIN1 and AZIN2) are homologues of ODC but devoid
25 of enzymatic activity. Little is known about *Xenopus* ODC and its paralogues, in spite of the
26 relevance of *Xenopus* as a model organism for biomedical research. We have used the
27 information existing in different genomic databases to compare the functional properties of the
28 amphibian ODC1, AZIN1 and AZIN2/ODC2, by means of transient transfection experiments
29 of HEK293T cells. Whereas the properties of xlODC1 and xLAZIN1 were similar to those
30 reported for their mammalian orthologues, xLAZIN2/xlODC2 showed important differences
31 with respect to human and mouse AZIN2. xLAZIN2 did not behave as an antizyme inhibitor,
32 but it rather acts as an authentic decarboxylase forming cadaverine, due to its affinity for L-
33 lysine as substrate; so, in accordance with this, it should be named as lysine decarboxylase
34 (LDC). In addition, AZ1 stimulated the degradation of xLAZIN2 by the proteasome, but the
35 removal of the 21 amino acid C-terminal tail, with a sequence quite different to that of mouse
36 or human ODC, made the protein resistant to degradation. Collectively, our results indicate that
37 in *Xenopus* there is only one antizyme inhibitor (xLAZIN1) and two decarboxylases, xlODC1
38 and xLLDC, with clear preferences for L-ornithine and L-lysine, respectively.

39

40

41 .

42

43 **Introduction**

44 Ornithine decarboxylase (ODC) is a rate-limiting enzyme in the polyamine biosynthetic
45 pathway that catalyzes the formation of putrescine from L-ornithine [1]. The polyamines
46 spermidine and spermine, and their precursor putrescine, are organic cations that interact with
47 different macromolecules, such as nucleic acids and proteins, affecting numerous cellular
48 mechanisms related to cell growth and differentiation, signal transduction, apoptosis and
49 autophagy [2–8]. In mammalian cells, ODC is highly regulated by a series of transcriptional,
50 translational and post-translational mechanisms [1, 9–11]. Interestingly, ODC is a short-lived
51 protein, with a half-life of less than 60 min in most mammalian tissues, and one of the few
52 proteins that are degraded by the proteasome without ubiquitination [12, 13]. In addition, in
53 the degradation of mammalian ODC, the antizyme 1 (AZ1) plays an important role [9, 14–16].
54 This regulatory protein is induced by increased levels of polyamines through an unusual
55 ribosomal frame-shifting mechanism in the translation of AZ1 mRNA [17, 18]. AZ1 binds to
56 the ODC monomer preventing the formation of the active ODC homodimer, and accelerates
57 the proteasomal degradation of ODC, presumably by inducing the exposure of a cryptic
58 proteasome-interacting surface of ODC [19]. The effects of antizymes on ODC are neutralized
59 by antizyme inhibitors (AZINs), protein homologues of ODC but lacking decarboxylase
60 activity [20–22]. In mammals, two AZINs have been identified (AZIN1 and AZIN2) that differ
61 in their tissue expression profile [22–25]. In contrast to ODC, the degradation of these proteins
62 is ubiquitin-dependent and is decreased by binding to AZ1 [26, 27].

63 Most studies on the structure, function and expression of ODC, AZs and AZINs have been
64 carried out with the human and rodent versions of these proteins, and in less extension with the
65 yeast and protozoan orthologues [28–31]. *Xenopus laevis* and *Xenopus tropicalis* are clawed
66 frogs that have been used as model organisms in developmental biology. However, little is
67 known about polyamine metabolism in these two species, and most of these studies have been

68 focused on the changes in ODC activity and polyamine levels during *Xenopus laevis* oogenesis
69 [32–34]. By screening a cDNA library from *Xenopus laevis* eggs, a cDNA corresponding to
70 ODC (XLODC1) was isolated and sequenced [35]. Later, a new paralogue of ODC from
71 *Xenopus laevis* (named xODC2) was identified, and the study of its temporal and spatial
72 expression pattern during early embryogenesis showed that this is quite different from that of
73 xLODC1 [36]. In addition, whereas transfection studies of ODC-deficient mutant C55.7 CHO
74 cells with XLODC1 showed that the *Xenopus* enzyme was functional in this heterologous
75 cellular model [33], to our knowledge, no data on the activity and properties of xODC2 are
76 available. In the Ensembl and Xenbase genome databases three *Xenopus* ODC paralogues are
77 annotated: ODC1, AZIN1 and AZIN2. xAZIN2 gene is also named as xODC2, but it is unclear
78 whether the corresponding protein functions as an antizyme inhibitor or alternatively it is an
79 authentic ornithine decarboxylase. Due to the remarkable properties of mouse AZIN2 found in
80 our previous studies [37–42], it appears relevant to analyze the characteristics of its amphibian
81 orthologue to determine whether this protein functions as an enzyme or as an antizyme
82 inhibitor. In the present work, we have transfected HEK293T cells with expression vectors
83 containing the ORF corresponding to xAZIN2, xODC1, and xAZIN1, and the enzymatic
84 activities and polyamine levels of these transfected cells were compared with those transfected
85 with their murine counterparts. We also analyzed the degradation of the *Xenopus* ODC
86 homologues and the effect of AZ1 on this process. Our results indicate that in *Xenopus laevis*,
87 in contrast to mammalian cells, there are two different decarboxylases of ornithine and lysine,
88 and only one protein acting as an antizyme inhibitor.

89 **Materials and methods**

90 **Materials**

91 L-[1-¹⁴C] ornithine and L-[1-¹⁴C] lysine were purchased from American Radiolabeled
92 Chemicals Inc. (St. Louis, MO, USA). Anti-Flag M2 monoclonal antibody peroxidase
93 conjugate (A8592), goat Anti-Rabbit IgG antibody peroxidase conjugated (AP132P), EDTA,
94 Igepal CA-630, cycloheximide, L-lysine, putrescine dihydrochloride, cadaverine
95 dihydrochloride, spermidine trihydrochloride, spermine tetrahydrochloride, 1,6-
96 hexanodiamine, 1,7-diaminoheptane, dansyl chloride, proteasome inhibitor MG-132 and
97 protease inhibitor cocktail (containing 4-(2-aminoethyl)benzenesulfonyl fluoride, EDTA,
98 bestatin, E-64, leupeptin, aprotinin) were obtained from Sigma Aldrich (St. Louis, MO).
99 Lipofectamine 2000 transfection reagent, Dulbecco's Modified Eagle Medium (DMEM
100 GlutaMAX), foetal bovine serum (FBS) and penicillin/streptomycin were purchased from
101 Invitrogen (Carlsbad, CA). Pierce ECL Plus Western Blotting Substrate was from
102 ThermoScientific (IL, USA). Rabbit anti-ERK2 antibody (SC-154) was purchased from Santa
103 Cruz Biotechnology (Texas, USA). The Anti-DYKDDDDK G1 Affinity Resin and the
104 DYKDDDDK peptide were obtained from GenScript. D,L-alpha-difluoromethylornithine
105 (DFMO) was provided by Dr. Patrick Woster (Medical University of South Carolina,
106 Charleston, SC). Gene and protein sequences were obtained from Xenbase
107 (<http://www.xenbase.org/>, [RRID:SCR_003280](#)) and Ensembl (www.ensembl.org) genome
108 databases.

109 **Cell culture and transient transfections**

110 Human embryonic kidney cells (HEK293T), obtained from ATCC, were cultured in DMEM
111 (Dulbecco's modified Eagle's medium), supplemented with 10% (v/v) fetal bovine serum, 100
112 units/ml penicillin, and 100 µg/ml streptomycin, in a humidified incubator containing 5% CO₂
113 at 37°C. Cells were grown to ~80% confluence and then were transiently transfected with
114 Lipofectamine 2000 using 1.5 µl of reagent and 0.3 µg of plasmid per well (12-well plates). In
115 co-transfection experiments, the mixtures contained equimolecular amounts of each construct.

116 The plasmid pcDNA3 without gene insertion was used as negative control. After 6 h of
117 incubation, the transfection medium was removed, fresh complete medium was added, and
118 cells were grown for additional 16 hours. Cells were collected and homogenized as described
119 below, whereas the culture media was used for polyamine analysis. In some cases, xLAZIN2
120 and xLODC1 were purified from the cell extracts by affinity chromatography using an anti-Flag
121 resin (GenScript) in accordance with the instructions of the supplier. All the constructs used in
122 transient transfections were cloned into the expression vector pcDNA3.1. The Flag epitope
123 DYKDDDDK was added to the N terminus of xLODC1, xLAZIN1, xLAZIN2, xLAZIN2 Δ C,
124 xLAZIN2-mAZIN2, mODC and mAZIN2 and to the C terminus of functional isoforms of
125 murineAZ1, AZ2 and AZ3. All the clones were generated and purchased from GenScript, and
126 sequenced before use.

127 **Western blot analysis**

128 Transfected HEK293T cells were collected in phosphate buffered saline (PBS), pelleted, and
129 lysed in solubilization buffer (50 mM Tris-HCl pH 8, 1% Igepal and 1 mM EDTA) with
130 protease inhibitor cocktail (Sigma Aldrich). The cell lysate was centrifuged at 14,000 \times g for 20
131 min. Equal amounts of protein were separated in 10% SDS-PAGE. The resolved proteins were
132 electroblotted to PVDF membranes, and the blots were blocked with 5% non-fat dry milk in
133 PBS-T (Tween 0.1%) and incubated overnight at 4 °C with the anti-Flag antibody conjugated
134 to peroxidase (1:10000). Immunoreactive bands were detected by using ECL Plus Western
135 Blotting Substrate. ERK2, detected by a rabbit anti-ERK2 antibody (Santa Cruz, USA), was
136 used as loading control. Densitometric analysis was achieved with ImageJ software.

137 **Enzymatic measurements**

138 Transfected HEK293T cells were collected in phosphate buffered saline (PBS), pelleted and
139 lysed in solubilization buffer (50mMTris-HCl, 1% Igepal and 1mM EDTA). After

140 centrifugation at 14,000 ×g for 20 min, 5µl of the supernatant were taken to a final volume of
141 50µl with buffer containing 10 mM Tris-HCl, 0.25M sucrose, 0.1 mM pyridoxal phosphate,
142 0.2 mM EDTA and 1 mM dithiothreitol. Decarboxylating activity was assayed in the
143 supernatant by measuring ¹⁴CO₂ released from L-[1-¹⁴C] ornithine or L-[1-¹⁴C] lysine. The
144 reaction was performed in glass tubes with tightly closed rubber stopper, hanging from the
145 stoppers two disks of filter paper wetted in 0.5 M benzethonium hydroxide, dissolved in
146 methanol. The samples were incubated at 37°C from 15 to 120 minutes, and the reaction was
147 stopped by adding 0.5 ml of 2 M citric acid. The filter paper disks were transferred to
148 scintillation vials, and counted for radioactivity in liquid-scintillation fluid. In some cases, the
149 enzyme activity was calculated by measuring by HPLC the rate of diamine formation
150 (putrescine or cadaverine), after incubation of the cell extracts with different concentration of
151 L-ornithine or L-lysine.

152 **Polyamine analysis**

153 Both intracellular polyamines and polyamines generated in the culture media of the transfected
154 cells were measured by HPLC. Transfected HEK293T cells were collected in phosphate
155 buffered saline (PBS), pelleted, and the polyamines were extracted from the cells by treatment
156 with 0.4M perchloric acid. The supernatant obtained after centrifugation at 10,000xg for 10
157 min was used for polyamine determination. For extracellular polyamine analysis, a fraction of
158 the cell culture media was concentrated with a Speedvac Concentrator (Savant Instruments Inc.
159 Farmingdale, NY, USA), and the resulting residue was resuspended in 0.4 M perchloric acid
160 and processed as described above. Polyamines from the acid supernatant were dansylated
161 according to a standard method [43]. Dansylated polyamines were separated by HPLC using a
162 BondaPak C18 column (4.6 x 300 mm; Waters) and acetonitrile/water mixtures (running from
163 70:30 to 96:4 during 30 min of analysis) as mobile phase and at a flow rate of 1 ml/min. 1,6-
164 Hexanediamine and 1,7-heptanediamine were used as internal standards. Detection of the

165 derivatives was achieved using a Waters 420-AC fluorescence detector, with a 340 nm
166 excitation filter and a 435 nm emission filter.

167 **Confocal microscopy**

168 Cells grown on coverslips were transfected with xlAzin2, xlOdc1, xlAzin1, mAzin2 or mOdc
169 constructs. Twenty-four hours after transfection, cells were fixed with 4% paraformaldehyde
170 in PBS and permeabilized with 0.5% Igepal in PBS. For detection of Flag-labelled proteins,
171 cells were incubated with an anti-Flag M2 monoclonal antibody (1:7.000), followed by an
172 Alexa 488-conjugated secondary antibody (1:400). For the staining of nucleus, cells were
173 loaded with DAPI (1:10000) for 5 minutes. Finally, samples were mounted by standard
174 procedures, using a mounting medium from Dako (Carpinteria) and examined with a Leica
175 True Confocal Scanner TCS-SP2 microscope.

176 **Statistical analysis**

177 The data were analyzed by Student's t-test for differences between means. $P < 0.05$ was
178 considered as statistically significant.

179

180 **Results**

181 **Comparative study of gene and protein structure of *Xenopus***

182 **AZIN2 with its paralogues and mammalian orthologues**

183 According to the Xenbase genome browser, the gene structures of Azin2 described for *Xenopus*
184 *tropicalis* (XB-GENE-6454420) and *Xenopus laevis* (XB-GENE-6493979) are similar. The
185 comparison of protein sequences between *Xenopus tropicalis* AZIN2 (xtAZIN2)
186 (NP_001015993.2) and *Xenopus laevis* AZIN2 (xlAZIN2) (NP_001079692.1), by using the

187 Clustal omega sequence alignment program, revealed a high homology (93.64%) (S1 Fig).
188 Since our preliminary experiments showed that both proteins behave similarly, we selected
189 *Xenopus laevis* for most experiments.

190 Next, we compared the gene structure of *Xenopus laevis* Odc paralogues with their respective
191 murine and human orthologues. Fig 1 shows that the xlAzin2 gene, like mouse Azin2 (mAzin2)
192 and human AZIN2 (hAZIN2), is formed by 11 exons (9 of them are coding exons), whereas
193 xlOdc and xlAzin1 contain 12 exons (10 coding exons), similarly to their murine and human
194 orthologues. The protein homology between the different orthologues of *Xenopus laevis* and
195 mice was analyzed by using the Align Sequences Protein BLAST (NCBI), and the results are
196 shown in Table 1. The sequence homology of xlAZIN2 with respect to xlODC1 or mODC was
197 higher (65% and 63%, respectively) than that of mAZIN2 (59%). In addition, sequence
198 similarity of mODC to xlODC1 was higher (82%) than that of xlAZIN2 (65%). The lowest
199 identity of xlAZIN2 was with xlAZIN1 (43%). These results indicate that although the genetic
200 structure of xlAzin2 is close to its mammalian orthologues, its protein sequence is closer to that
201 of *Xenopus* or mouse ODC proteins.

202 **Fig 1. Genetic structure of mouse and human ODC paralogues, and their comparison**
203 **with their *Xenopus* orthologues.** Note that exons 7 and 8 in ODC and AZIN1 are fused in
204 only one exon in AZIN2 (blue boxes). Data obtained from Ensembl (www.ensembl.org).

205 **Table 1. Sequence identity between mouse (m) and *Xenopus laevis* (xl) homologue**
206 **proteins.**

207

	xlAZIN2	xlODC1	xlAZIN1	mAZIN2	mODC	mAZIN1
xlAZIN2	100	65	43	59	63	49
xlODC1	65	100	47	52	82	51
xlAZIN1	43	47	100	42	46	67

208 Fig 2 shows the sequence alignment of the proteins corresponding to the three ODC paralogues
209 of *Xenopus laevis* (xlODC1, xLAZIN1 and xLAZIN2) and mODC. The amphibian xLAZIN2, as
210 xlODC1, shares with mODC the 22 residues that are required for the decarboxylating activity
211 [40, 44–48] whereas xLAZIN1, as reported for mammalian AZIN1 and AZIN2, lacks some
212 essential residues such as K69 and C360. These results indicate that, according to these putative
213 catalytic residues, xLAZIN2 appears to be closer to ODCs than to AZINs. Fig 2 also shows that
214 lower homologies were found in the ~70 amino acids residues of the C-terminal region. The
215 identity values of mODC with respect to xlODC1, xLAZIN2 and xLAZIN1 were 63%, 31% and
216 17%, respectively (S1 Table). Since two adjacent segments in the C-terminal region of ODC
217 (segments S1 and S2 in S2 Fig), have been proposed as having different roles in the
218 proteasomal degradation of ODC induced by AZ1 [19], we also calculated the sequence
219 homology in these segments among the different ODC homologues (S2 Fig). S1 Table also
220 shows that the identity values among S1 segments from mODC and its amphibian homologues
221 (77%, 44% and 26%) were higher than those corresponding among the S2 segments (66%,
222 14% and 9%).

223 **Fig 2. Comparison of the amino acid sequences of mouse ODC, xlODC1, xLAZIN1 and**
224 **xLAZIN2 using ClustalW program for multiple sequence alignment.** Asterisks represent
225 amino acid identity; colon and dots represent amino acid similarity between the proteins. Grey
226 background indicates amino acid residues associated with the catalytic activity of mODC that
227 are conserved in the *Xenopus laevis* homologues. In red: substitutions in these critical residues
228 in xLAZIN1.

229

230 **Functional analysis of xLAZIN2 in a heterologous cell system.**

231 To test the potential ornithine decarboxylase activity of xLAZIN2, HEK293T cells were
232 transiently transfected with xLAZIN2, and the decarboxylating activity was measured in
233 homogenates from the transfected cells. In parallel, cells were also transfected with the empty
234 vector and with plasmids containing the coding sequences of xLODC1 and xLAZIN1, in the
235 same vector as xLAZIN2. As displayed in Fig 3A, the homogenates from cells transfected with
236 xLODC1 showed, as expected, a high ODC activity in comparison to those from mock
237 transfected cells. In the case of xLAZIN2, the ODC activity was about 22% of the values found
238 for xLODC1, and much higher than that of xLAZIN1. Western blot analysis revealed that these
239 differences in ODC activity were not due to significant differences in protein expression levels.
240 Both xLODC1 and xLAZIN2 were inhibited by treatment of the cells with 1 mM DFMO (Fig
241 3B). These results suggested that either xLAZIN2 is an antizyme inhibitor more potent than
242 xLAZIN1 for increasing the endogenous ODC activity, or that it may possess intrinsic catalytic
243 activity.

244 **Fig 3. Expression of xLODC1, xLAZIN1 and xLAZIN2 in HEK293T transfected cells.**

245 HEK293T cells were transfected with the corresponding constructs of Flag-xLODC1, Flag-
246 xLAZIN1, Flag-xLAZIN2 or empty vector, as indicated in the Experimental Procedures. (A)
247 Top: ODC activity measured in the cell lysates. Bottom: Western blot analysis of the proteins
248 detected using anti-Flag or anti-ERK2 antibodies. Results are expressed as mean \pm SE, and are
249 representative of three experiments. (**) $P < 0.01$ vs pcDNA3 or X-xLODC1. (B) Influence of
250 1mM alfa-difluoromethylornithine (DFMO) on the ornithine decarboxylase activity of
251 xLODC1 and xLAZIN2 cell lysates. (*) $P < 0.05$.

252

253 To corroborate the latter possibility, we next analyzed the influence of xLAZIN2 on polyamine
254 levels. For that purpose, we studied the influence of xLAZIN2 transfection on the polyamine
255 content of the transfected cells and on that of the culture media, after 16 h of the transfection.

256 Fig 4A shows the chromatogram traces of the dansylated polyamines obtained by HPLC
257 analysis of HEK293T homogenates from cells transfected with xIAZIN2 or with the empty
258 vector. A dramatic increase in putrescine levels was evident after transfection with xIAZIN2.
259 Unexpectedly, the major increment was observed for cadaverine, the diamine that is produced
260 by decarboxylation of L-lysine, with values about 3-fold higher than those of putrescine. The
261 analysis of the polyamine content of the culture media of the xIAZIN2-transfected cells also
262 showed that cadaverine was the most abundant polyamine, with values about 10-fold higher
263 than those of putrescine (Fig 4B). The finding that the cadaverine to putrescine ratio in the cell
264 cultures was about 3-fold higher than the diamine ratio in the cell extracts revealed that
265 cadaverine is excreted more efficiently than putrescine in this type of cells.

266 **Fig 4. Analysis of the products formed by HEK293T cells transfected with different**
267 **constructs.** After 16 h of transfection, the culture media was aspirated and the cells collected.
268 An aliquot of the media was concentrated and resuspended in perchloric acid 0.4 M, whereas
269 the cells were homogenized in the same acid (200 μ l per well). After centrifugation at 12.000
270 \times g for 15 min, the supernatants were dansylated and analyzed by HPLC as described in the
271 Experimental section. (A) Overlapped HPLC chromatogram traces of the dansylated extracts
272 from cells transfected with xIAZIN2 (red line) or with the empty vector pcDNA 3.1 (blue line).
273 Hexanediamine (Hxd) and heptanediamine (Hpd) were used as internal standards. Put:
274 putrescine; Cad: cadaverine; Spd: spermidine; Spm: spermine. (B) Overlapped HPLC
275 chromatogram traces corresponding to the dansylated polyamines present in the culture media
276 of cells transfected with xIAZIN2 (red line) or empty vector (blue line). (C) Comparison of the
277 polyamines found in the culture media of cells transfected with xIAZIN2 (red line) with those
278 of xLODC1, mODC and mAZIN2 (blue line).

279

280 Since it is known that mouse and rat ODCs are able to decarboxylate L-lysine, but less
281 efficiently than L-ornithine [49], we compared the levels of putrescine and cadaverine in cells
282 transfected with xlAZIN2 with those of the cells transfected with xlODC1, mODC or mAZIN2.
283 Figs 4C and 4D show that the ratio cadaverine:putrescine in the cells transfected with any of
284 the two ODCs were lower than one, whereas in the case of xlAZIN2 this ratio was higher than
285 7. These results indicate that xlAZIN2 is more efficient to synthesize cadaverine than
286 putrescine under the cell culture conditions employed in the assays. In addition, in the cells
287 transfected with mAZIN2, only vestigial levels of cadaverine were detected, whereas
288 putrescine levels were similar to those of xlAZIN2 transfected cells (Fig 4E). All these results
289 clearly indicated that xlAZIN2 behaves as an enzyme that can decarboxylate both amino acids
290 L-ornithine and L-lysine to produce putrescine and cadaverine, respectively.

291 **Kinetic analysis of the decarboxylase activity of xlAZIN2**

292 The enzyme kinetic parameters were analyzed using cell homogenates from xlAZIN2- or
293 xlODC1-transfected HEK293T cells and different substrate concentrations. Table 2 shows that
294 in the case of xlAZIN2 the K_m for L-lysine (1.06 ± 0.25 mM) was lower than the K_m for L-
295 ornithine (6.57 ± 1.75 mM), suggesting that the affinity of xlAZIN2 to L-lysine is higher than
296 the one to L-ornithine. The opposite was found for xlODC1, although here the affinity of
297 xlODC1 for L-ornithine was much higher than for L-lysine ($K_m^{Orn} = 0.023 \pm 0.008$ mM and
298 $K_m^{Lys} = 30.1 \pm 7.8$ mM). Taking the ratio V_m/K_m as an indicator of the catalytic efficiency of
299 each enzyme, the results presented in Table 2 indicate that xlAZIN2 was much more efficient
300 to decarboxylate L-lysine than xlODC1, whereas the opposite was found when L-ornithine was
301 the substrate. In parallel experiments, using enzymes purified by affinity chromatography with
302 anti-Flag beads, the K_m values found were essentially similar to those presented in Table 2.

303 **Table 2. Comparison of the kinetic parameters of xlAZIN2 and xlODC1.**

304

305

Substrate	L-ornithine			L-lysine		
	Km (mM)	Vm	Vm/Km	Km (mM)	Vm	Vm/Km
xIAZIN2	6.57±1.75	119±23	18.1	1.06±0.25	24.7±2.3	23.3
xIODC1	0.023±0.01	2.85±0.29	124	30.1±7.8	4.67±0.84	0.15

306

307 Vm is expressed as nmol of product formed per h and 10⁶ cells. The ratio Vm/Km is
308 expressed in arbitrary units.

309

310 **Study of a possible antizyme inhibitory action of xIAZIN2.**

311 Although all above results clearly supported that xIAZIN2 has decarboxylating activity, it
312 could be likely that xIAZIN2 may also act as an antizyme inhibitor. To test this possibility, we
313 analyzed the ability of xIAZIN2 to rescue xIODC1 from the predictable degradation induced by
314 AZ1, as early reported for mouse AZIN2 [37]. To this purpose, we carried out different co-
315 transfection experiments using several constructs. The results shown in Fig 5A corroborated
316 that, as expected, AZ1 stimulated the degradation of xIODC1, and that none of the two
317 xIAZIN2 constructs used (either with Flag for western blot detection or without Flag) were
318 able to protect xIODC1 from degradation. In addition, the results shown in this figure also
319 suggested that xIAZIN2 was induced to degradation by AZ1. To confirm this possibility,
320 xIAZIN2 was co-transfected with AZ1, and the cell homogenates were analyzed for
321 decarboxylase activity and xIAZIN2 protein content. Fig 5B clearly shows that AZ1 induced
322 the degradation of xIAZIN2. Taking into consideration that earlier studies showed that mouse
323 AZIN2 protected mouse ODC from degradation, whereas it was not degraded by AZ1 [37], the
324 results shown here do not support a role of xIAZIN2 as an antizyme inhibitor. On the contrary,

325 similar experiments using xIAZIN1 showed that AZ1, as it is known for mAZIN1 [26],
326 protected the amphibian protein from degradation (S3 Fig).

327 **Fig 5. Influence of AZ1 on protein levels of xLODC1 and xIAZIN2.** (A) Western blot of
328 lysates of HEK293T cells co-transfected with xLODC1 and different combinations of AZ1 and
329 xIAZIN2. (B) Western blot and ODC activity of lysates of cells co-transfected with Flag-
330 xIAZIN2 and pcDNA3 or AZ1. (***) $P < 0.001$ vs pcDNA3 or F-xIAZIN2+AZ1.

331

332 Furthermore, the subcellular distribution of xIAZIN2 in the transfected cells was found to be
333 mainly cytosolic, similar to that of xLODC1 or mODC, and different from that of mAZIN2 (Fig
334 6). All these results demonstrate that the gene annotated as xIAZIN2 in the different gene
335 databanks does not code for a *bona fide* antizyme inhibitor, but instead it encodes for an
336 authentic amino acid decarboxylase with preference for L-lysine as substrate. Therefore, we
337 propose to change its name to lysine decarboxylase (LDC).

338 **Fig 6. Subcellular location of xLODC1 and xIAZIN2 in transfected cells.** Laser scanning
339 confocal micrographs of HEK293T cells transfected with xLODC1, xIAZIN2, mODC or
340 mAZIN2 fused to the Flag epitope. After transfections, cells were fixed, permeabilized and
341 stained with anti-Flag antibody and ALEXA anti-mouse and nuclear DAPI staining, and then
342 examined in a confocal microscope. Flag-proteins are shown in green and nuclei in blue.

343

344 **Degradation of xIAZIN2 in HEK293T cells**

345 The half live of xIAZIN2 was calculated by measuring the decay in both enzymatic activity
346 and protein content (estimated by western-blotting), after inhibition of protein synthesis by
347 cycloheximide treatment. Fig 7A shows that xIAZIN2 is a short-lived protein ($t_{1/2} \sim 34$ min)
348 with a metabolic turn-over higher than that of xLODC1 ($t_{1/2} \sim 136$ min), under the same

349 analytical conditions (Fig 7B). In addition, the great reduction in the degradative rate elicited
350 by treatment with MG132, a potent inhibitor of proteasomal degradation, shown by Fig 7C,
351 suggests that xLAZIN2 can be degraded by the mammalian proteasome in a similar way to that
352 of their mammalian orthologues.

353 **Fig 7. Protein stability of xLAZIN2 and xLODC1 in transfected cells.** After 16 h of
354 transfection, either with xLAzin2 or xLOdc1, cells were incubated with 200 μ M cycloheximide
355 (CHX), harvested at the indicated times, and lysed in buffer containing a protease inhibitor
356 cocktail. (A) Left: Western blot analysis of xLAZIN2 protein using the anti-Flag antibody; right:
357 decay of ODC activity. (B) Similar experiments with xLODC1. Half-lives of xLAZIN2 and
358 xLODC1 in the transfected cells were calculated by linear regression analysis (GraphPad
359 software). (C) HEK293T cells transfected with xLAZIN2 or xLAZIN2+AZ1 were incubated for
360 5 h with or without the proteasomal inhibitor MG132 (50 μ M). xLAZIN2 protein was
361 determined as in (A). ERK2 was used as a loading control.

362

363 Since it is very well known that the last 37 amino acid residues of the carboxyl terminus of
364 mammalian ODC play a relevant role in its rapid intracellular degradation [50, 51], we decided
365 to analyze the relevance of this C-terminal region in the amphibian protein on the degradation
366 of xLAZIN2. For that purpose, we generated two mutated versions of xLAZIN2 and studied the
367 influence of the different antizymes (AZ1, AZ2, and AZ3) in the degradation of wild type
368 xLAZIN2, and in that of its C-terminal mutant forms, in the HEK293T-transfected cells. The
369 first xLAZIN2 mutant was a truncated form in which the last 21 amino acid residues of the C-
370 term of xLAZIN2 were deleted (xLAZIN2- Δ C). This deleted sequence
371 (CGWEISDSLCFTRTFAATSII) has a poor homology (14%) with the corresponding one in
372 mODC (CAQESGMDRHPAACASARINV). The second mutant was a quimeric protein
373 (xLAZIN2-mAZIN2) in which the mentioned C-terminal sequence in xLAZIN2 was substituted

374 by the corresponding C-terminal region of mAZIN2 (CGWEITDTLCVGPVFTPASIM). Fig
375 8A shows that, whereas AZ1, as earlier shown, increased the degradation of xLAZIN2, AZ2
376 and AZ3 did not stimulate the degradation of this protein. On the opposite, the truncation of
377 the C-terminal region of the protein prevented its AZ1-dependent degradation, indicating that
378 the 21 amino acid residues of the C-terminal region of xLAZIN2, as in the case of mODC, play
379 a relevant role in the degradative process. Again, as in the case of xLAZIN2, the stability of the
380 truncated protein was not significantly affected by any of the other two antizymes (Fig 8B).
381 Moreover, as shown in Fig 8C, the quimeric protein xLAZIN2-mAZIN2 showed against
382 antizymes a behavior similar to that found for xLAZIN2. This indicated that the substitution of
383 the C-terminal of xLAZIN2 by the corresponding region from mAZIN2, did not protect this
384 quimeric protein from the antizyme-induced degradation. Figs 9A and 9B also show that the
385 deletion of the C-terminal region of xLAZIN2 prevented its rapid degradation. The fact that
386 degradation of the quimeric protein xLAZIN2-mAZIN2 was decreased by MG132 (Fig 9C), as
387 already shown by the wild type protein (Fig 7C), suggested that the proteasome participates in
388 the degradation of both proteins.

389 **Fig 8. Influence of the C-terminal region of xLAZIN2 in the degradative process induced**
390 **by AZs.** HEK293T cells were transfected with: (A) xLAZIN2, (B) xLAZIN2 lacking the 21 C-
391 terminal residues (xLAZIN2- Δ C) or (C) with a construct coding for a quimeric protein with the
392 substitution of the 21 C-terminal residues of xLAZIN2 by the C-terminal segment of mouse
393 AZIN2 (xLAZIN2-mAZIN2). In parallel, each one of the constructs was co-transfected with
394 members of the AZ family (AZ1, AZ2, and AZ3). Western-blot were probed with anti-Flag
395 antibody. On the right side, schematic representations of xLAZIN2 and the two mutated
396 proteins.

397 **Fig 9. Protein stability of the mutated forms of xLAZIN2.** (A) After 16 h of transfection with
398 xLAZIN2- Δ C, cells were incubated with 200 μ M cycloheximide (CHX), harvested at the

399 indicated times, and lysed in buffer containing a protease inhibitor cocktail. Top: western blot
400 analysis of xIAZIN2- Δ C at different times after CHX addition; bottom: changes in ODC
401 activity after CHX treatment. (B) Influence of the proteasomal inhibitor MG132 (50 μ M) on
402 the effect of AZ1 on xIAZIN2- Δ C protein in HEK293T transfected cells. (C) Influence of the
403 proteasomal inhibitor MG132 (50 μ M) on the effect of AZ1 on xIAZIN2-mAZIN2 protein in
404 HEK293T transfected cells.

405 **Discussion**

406 Our results clearly indicate that xIAZIN2 is devoid of antizyme inhibitory capacity, since it
407 was unable to rescue ODC from the negative effect of AZ1 (Fig 5A). In addition, AZ1 did not
408 protect xIAZIN2 from degradation (Figs 5B and 7C), contrary to what was reported for
409 mAZIN1 and mAZIN2 [26, 37]. Unexpectedly, AZ1 accelerated the degradation of xIAZIN2
410 by the proteasome (Fig 7C), as it was also observed for xLODC1 (Fig 5A), and as early
411 described for mammalian ODCs [14, 52].

412 On the contrary, our findings unambiguously demonstrated that xIAZIN2 was able to
413 decarboxylate not only L-ornithine but also L-lysine, producing the diamines putrescine and
414 cadaverine, respectively (Figs 4A and 4B). It was also clear that in the cultured cells transfected
415 with either xLODC1 or mODC, cadaverine was also produced but in a lesser amount than
416 putrescine (Figs 4C and 4D). These results are in agreement with early reports that showed that
417 ODC from rodent tissues was able to decarboxylate both amino acids, although L-lysine less
418 efficiently than L-ornithine [49]. The comparison of the kinetic parameters of xIAZIN2 with
419 those of xLODC1 showed that the affinity of xIAZIN2 for lysine is about 30-fold higher than
420 that of xLODC1, whereas the opposite was evident for ornithine. All these results reveal that
421 in *Xenopus laevis* there are two related genes (xLODC1 and xIAZIN2) coding for enzymes able
422 to decarboxylate both amino acids ornithine and lysine. Whereas the function of xLODC1

423 appears to be related with the formation of putrescine, and therefore in consonance with that of
424 mammalian ODCs, our data suggest that it is very likely that the main role of xLAZIN2 could
425 be concerned with the synthesis of cadaverine. Although some studies revealed the presence of
426 cadaverine in several amphibian tissues [53, 54], including those adult *Xenopus laevis* during
427 limb regeneration [55], the physiological function of this diamine is mostly unknown. Taking
428 into consideration that the protein sequence of xLAZIN2 is identical to that reported for xLODC2
429 [36], it can be assumed that xLODC2 may have lysine decarboxylase activity, although it should
430 be noted that no enzymatic activity for xLODC2 was measured in the mentioned report.
431 Interestingly, it was also reported that xLODC1 and xLODC2 showed different expression
432 patterns during *Xenopus laevis* embryo development [36]. The specific regional and temporal
433 expression of xLODC2 during specific stages of *Xenopus* embryo development [36], associated
434 to the mentioned lysine decarboxylase activity of xLODC2, suggest that cadaverine may have
435 some role during *Xenopus* embryogenesis, different to that of putrescine. This possibility could
436 also explain the reason for the existence of two apparently similar ODC decarboxylases in
437 *Xenopus*.

438 According to our results, the two *Xenopus* enzymes xLODC1 and xLODC2/xLAZIN2 expressed
439 in mammalian cells share several properties with mouse ODC, such as their cytosolic
440 localization, short half-lives, and AZ1-stimulated degradation by the proteasome. On the other
441 hand, xLODC2/xLAZIN2 differs from mAZIN2 in that the murine protein lacks decarboxylase
442 activity and is located in vesicular-like structures, and that AZ1 protects mAZIN2 from
443 degradation [37, 56, 57]. The mechanisms by which AZs exert opposite effects on the protein
444 stability of ODC and AZINs are not completely understood. Different studies have
445 demonstrated that in ODC there are two regions participating in its rapid turn-over [revised in
446 58]. The first region encompasses amino acid residues 117-140 needed for AZ binding (AZBE
447 region) [52]. The second is the C-terminal region in mammalian ODC [59–61] or the N-

448 terminal region of yeast ODC [31]. Interestingly, our results showed that the deletion of the 21
449 amino acid residues of the C-terminal region of xLODC2/xLAZIN2 made the truncated protein
450 more stable and resistant to AZ1-induced degradation by the proteasome. This result is in
451 agreement with early reports showing that the truncation of the carboxyl-terminal segment of
452 mouse ODC prevented its rapid intracellular degradation [50, 59]. However, the substitution
453 of this C-terminal region in xLAZIN2 by the corresponding one of mAZIN2 did not protect it
454 from AZ1-induced degradation, despite being known that the degradation of mAZIN2 is not
455 stimulated by binding to AZ1 [27]. Taking into consideration the low sequence homology
456 between the 21 amino acid C-terminal tail of xLAZIN2 or that of the quimeric protein with that
457 of mODC (14% and 9%, respectively, as shown in S1 Table), our results support the contention
458 that different C-terminal amino acid sequences may lead to the interaction of these ODC
459 homologous proteins with the proteasome. According to current views, an unstructured
460 terminal domain can be absolutely essential as the initiation site for protein degradation [62,
461 63]. As shown here, in the case of xODC homologues, different C-tail sequences can
462 accomplish this requirement. Apart from the implication of this terminal protein segment (S2)
463 in the initial infiltration of the protein in the proteolytic chamber of the proteasome, recent
464 studies based on structural analyses have proposed that the interaction of ODC-AZ complex
465 with the proteasome requires the exposure of the ODC residues 391-420 [19]. However, the
466 specific role of the different amino acid residues within this pre-terminal sequence (S1) on the
467 interaction with the proteasome is still unknown. As shown in S1 Table, it is clear that the
468 homology of the S1 segment of xLODC1 and xLAZIN2/ODC2, the two amphibian proteins
469 induced to be degraded by AZ1, with that of mODC is higher than those calculated for xLAZIN1
470 or mouse AZINs, proteins whose degradation is not stimulated by AZ1. This finding supports
471 early conclusions based on structural studies that claimed for the relevance of the 391-420 ODC
472 region for interacting with the proteasome [19]. The existence of the invariable sequence

473 FNGFQ in the S1 segments of mODC, xlODC1 and xlAZIN2/ODC2 (S2 Fig), that according
474 to the above-mentioned structural study forms a short helical turn, suggests that this part of the
475 S1 terminal region may be critical for recognition by the proteasome. If this is the case, the
476 alteration of this sequence in the AZINs could make these proteins resistant to the degradative
477 stimulatory action of AZs.

478 Collectively, our study demonstrates, firstly, that xlAZIN2, although having a gene structure
479 similar to those of mammalian AZIN2s, is not really an antizyme inhibitor, but an authentic
480 decarboxylase with preference for L-lysine as substrate. According to this, the name of xLLDC
481 (or xlODC2), instead of xlAZIN2, should be used. Secondly, our results also extend the
482 previous knowledge on the influence of AZs on degradative aspects, from mammalian ODCs
483 to non-mammalian ODCs different from yeast or trypanosomal ODCs. Our findings support
484 the hypothesis that in the C-terminal region of *Xenopus* ODCs the last 21 amino acid tail is
485 required for antizyme-stimulated degradation of the enzyme, and suggest that the sequence
486 FNGFQ encompassing residues 396~400 may be relevant for the interaction of mammalian
487 and amphibian ODCs with the proteasome.

488

489

490

491

492

493

494

495 **References**

- 496 1. Pegg AE. Regulation of ornithine decarboxylase. *J Biol Chem.* 2006; 281(21): 14529-
497 14532. doi: 10.1074/jbc.R500031200.
- 498 2. Cohen S. *A Guide to the Polyamines.* 1997. Oxford, UK: Oxford University Press.
- 499 3. Igarashi K, Kashiwagi K. Polyamines: Mysterious modulators of cellular functions.
500 *Biochem Biophys Res Commun.* 2000; 271(3): 559-564. doi: 10.1006/bbrc.2000.2601.
- 501 4. Gerner EW, Meyskens FL. Polyamines and cancer: old molecules, new understanding.
502 *Nat Rev Cancer.* 2004; 4(10): 781-792. doi: 10.1038/nrc1454
- 503 5. Igarashi K, Kashiwagi K. Modulation of cellular function by polyamines. *Int J Biochem*
504 *Cell Biol.* 2010; 42(1): 39-51. doi: 10.1016/j.biocel.2009.07.009..
- 505 6. Minois N. Molecular basis of the “anti-aging” effect of spermidine and other natural
506 polyamines - A mini-review. *Gerontology.* 2014; 60(4): 319-326. doi: 10.1159/000356748.
- 507 7. Pegg AE. Functions of polyamines in mammals. *J Biol Chem.* 2016; 291(29): 14904-
508 14912. doi: 10.1074/jbc.R116.731661.
- 509 8. Bae DH, Lane DJR, Jansson PJ, Richardson DR. The old and new biochemistry of
510 polyamines. *Biochim Biophys Acta Gen Subj.* 2018; 1862(9): 2053-2068. doi:
511 10.1016/j.bbagen.2018.06.004.
- 512 9. Coffino P. Regulation of cellular polyamines by antizyme. *Nat Rev Mol Cell Biol.*
513 2001; 2: 188–194.
- 514 10. Kahana C. Antizyme and antizyme inhibitor, a regulatory tango. *Cell Mol Life Sci.*
515 2009; 66(15): 2479-88. doi: 10.1007/s00018-009-0033-3.

- 516 11. Miller-Fleming L, Olin-Sandoval V, Campbell K, Ralser M. Remaining Mysteries of
517 Molecular Biology: The Role of Polyamines in the Cell. *J Mol Biol.* 2015; 427(21): 3389-3406.
518 doi: 10.1016/j.jmb.2015.06.020.
- 519 12. Murakami Y, Matsufuji S, Kameji T, Hayashi SI, Igarashi K, Tamura T, et al. Ornithine
520 decarboxylase is degraded by the 26S proteasome without ubiquitination. *Nature.* 1992;
521 360(6404), 597-599. doi: 10.1038/360597a0
- 522 13. Erales J, Coffino P. Ubiquitin-independent proteasomal degradation. *Biochim Biophys*
523 *Acta - Mol Cell Res.* 2014; 1843(1): 216-221
- 524 14. Murakami Y, Matsufuji S, Hayashi SI, Tanahashi N, Tanaka K. Degradation of
525 ornithine decarboxylase by the 26S proteasome. *Biochem Biophys Res Commun.* 2000;
526 267(1):1-6.
- 527 15. Mangold U. The antizyme family: Polyamines and beyond. *IUBMB Life.* 2005; 57(10):
528 671-676. doi: 10.1080/15216540500307031.
- 529 16. Kahana C. The antizyme family for regulating polyamines. *J Biol Chem.* 2018;
530 293(48):18730-18735. doi: 10.1074/jbc.TM118.003339.
- 531 17. Rom E, Kahana C. Polyamines regulate the expression of ornithine decarboxylase
532 antizyme in vitro by inducing ribosomal frame-shifting. *Proc Natl Acad Sci.* 2006; 91(9), 3959-
533 3963.
- 534 18. Matsufuji S, Matsufuji T, Miyazaki Y, Murakami Y, Atkins JF, Gesteland RF, et al.
535 Autoregulatory frameshifting in decoding mammalian ornithine decarboxylase antizyme. *Cell.*
536 1995; 80(1): 51-60.

- 537 19. Wu H-Y, Chen S-F, Hsieh J-Y, Chou F, Wang Y-H, Lin W-T, et al. Structural basis of
538 antizyme-mediated regulation of polyamine homeostasis. *Proc Natl Acad Sci USA*. 2015;
539 112(36):11229-11234. doi: 10.1073/pnas.1508187112
- 540 20. Mangold U. Antizyme inhibitor: Mysterious modulator of cell proliferation. *Cell Mol*
541 *Life Sci*. 2006; 63(18):2095-2101. doi: 10.1007/s00018-005-5583-4
- 542 21. López-Contreras AJ, Ramos-Molina B, Cremades A, Peñafiel R. Antizyme inhibitor 2:
543 Molecular, cellular and physiological aspects. *Amino Acids*. 2010; 38: 603–611.
- 544 22. Ramos-Molina B, Lambertos A, Peñafiel R. Antizyme Inhibitors in Polyamine
545 Metabolism and Beyond: Physiopathological Implications. *Med Sci*. 2018. pii: E89. doi:
546 10.3390/medsci6040089.
- 547 23. Tang H, Arika K, Ohkido M, Murakami Y, Matsufuji S, Li Z, et al. Role of ornithine
548 decarboxylase antizyme inhibitor in vivo. *Genes to Cells*. 2009; 14: 79-87.
- 549 24. Ramos-Molina B, López-Contreras AJ, Cremades A, Peñafiel R. Differential
550 expression of ornithine decarboxylase antizyme inhibitors and antizymes in rodent tissues and
551 human cell lines. *Amino Acids*. 2012; 42: 539-547.
- 552 25. Rasila T, Lehtonen A, Kanerva K, Mäkitie LT, Haglund C, Andersson LC. Expression
553 of ODC Antizyme Inhibitor 2 (AZIN2) in Human Secretory Cells and Tissues. *PLoS One*.
554 2016; 11: e0151175. doi: 10.1371/journal.pone.0151175
- 555 26. Bercovich Z, Kahana C. Degradation of antizyme inhibitor, an ornithine decarboxylase
556 homologous protein, is ubiquitin-dependent and is inhibited by antizyme. *J Biol Chem*. 2004;
557 279(52): 54097-54102. doi: 10.1074/jbc.M410234200.

- 558 27. Snapir Z, Keren-Paz A, Bercovich Z, Kahana C. ODCp, a brain- and testis-specific
559 ornithine decarboxylase paralogue, functions as an antizyme inhibitor, although less efficiently
560 than AzII. *Biochem J.* 2008; 410: 613-619.
- 561 28. Ghoda L, Phillips MA, Bass KE, Wang CC, Coffino P. Trypanosome ornithine
562 decarboxylase is stable because it lacks sequences found in the carboxyl terminus of the mouse
563 enzyme which target the latter for intracellular degradation. *J Biol Chem.* 1990;
564 265(20):11823-11826.
- 565 29. Gupta R, Hamasaki-Katagiri N, Tabor CW, Tabor H. Effect of spermidine on the in
566 vivo degradation of ornithine decarboxylase in *Saccharomyces cerevisiae*. *Proc Natl Acad Sci*
567 *USA.* 2002; 98(19):10620-10623.
- 568 30. Porat Z, Landau G, Bercovich Z, Krutauz D, Glickman M, Kahana C. Yeast antizyme
569 mediates degradation of yeast ornithine decarboxylase by yeast but not by mammalian
570 proteasome: New insights on yeast antizyme. *J Biol Chem.* 2008; 283: 4528–4534.
571 doi:10.1074/jbc.M708088200.
- 572 31. Gödderz D, Schäfer E, Palanimurugan R, Dohmen RJ. The N-terminal unstructured
573 domain of yeast odc functions as a transplantable and replaceable ubiquitin-independent
574 degron. *J Mol Biol.* 2011; 407(3): 354-367. doi: 10.1016/j.jmb.2011.01.051.
- 575 32. Osborne HB, Mulner-Lorillon O, Marot J, Belle R. Polyamine levels during *Xenopus*
576 *laevis* oogenesis: A role in oocyte competence to meiotic resumption. *Biochem Biophys Res*
577 *Commun.* 1989; 158: 520-526.
- 578 33. Osborne HB, Duval C, Ghoda L, Omilli F, Bassez T, Coffino P. Expression and
579 post-transcriptional regulation of ornithine decarboxylase during early *Xenopus* development.
580 *Eur J Biochem.* 1991; 202: 575-581.

- 581 34. Osborne HB, Cormier P, Lorillon O, Maniey D, Belle R. An appraisal of the
582 developmental importance of polyamine changes in early *Xenopus* embryos. *Int J Dev Biol.*
583 1993; 37: 615-618.
- 584 35. Bassez T, Paris J, Omilli F, Dorel C, Osborne HB. Post-transcriptional regulation of
585 ornithine decarboxylase in *Xenopus laevis* oocytes. *Development.* 1990; 110: 955-962.
- 586 36. Cao Y, Zhao H, Hollemann T, Chen Y, Grunz H. Tissue-specific expression of an
587 Ornithine decarboxylase paralogue, XODC2, in *Xenopus laevis*. *Mech Dev.* 2001; 102: 243-
588 246.
- 589 37. López-Contreras AJ, López-García C, Jiménez-Cervantes C, Cremades A, Peñafiel R.
590 Mouse ornithine decarboxylase-like gene encodes an antizyme inhibitor devoid of ornithine
591 and arginine decarboxylating activity. *J Biol Chem.* 2006; 281(41): 30896-30906. doi:
592 10.1074/jbc.M602840200.
- 593 38. López-Contreras AJ, Ramos-Molina B, Martínez-de-la-Torre M, Peñafiel-Verdú C,
594 Puelles L, Cremades A, et al. Expression of antizyme inhibitor 2 in male haploid germinal cells
595 suggests a role in spermiogenesis. *Int J Biochem Cell Biol.* 2009; 41(5): 1070-1078. doi:
596 10.1016/j.biocel.2008.09.029.
- 597 39. López-García C, Ramos-Molina B, Lambertos A, López-Contreras AJ, Cremades A,
598 Peñafiel R. Antizyme Inhibitor 2 Hypomorphic Mice. New Patterns of Expression in Pancreas
599 and Adrenal Glands Suggest a Role in Secretory Processes. *PLoS One.* 2013; 8(7): e69188.
600 doi: 10.1371/journal.pone.0069188.
- 601 40. Ramos-Molina B, Lambertos A, López-Contreras AJ, Peñafiel R. Mutational analysis
602 of the antizyme-binding element reveals critical residues for the function of ornithine
603 decarboxylase. *Biochim Biophys Acta - Gen Subj.* 2013; 1830(11):5157-5165. doi:
604 10.1016/j.bbagen.2013.07.003.

- 605 41. Ramos-Molina B, Lambertos A, Lopez-Contreras AJ, Kasprzak JM, Czerwoniec A,
606 Bujnicki JM, et al. Structural and degradative aspects of ornithine decarboxylase antizyme
607 inhibitor 2. FEBS Open Bio. 2014; 4: 510-521. doi: 10.1016/j.fob.2014.05.004.
- 608 42. Lambertos A, Ramos-Molina B, López-Contreras AJ, Cremades A, Peñafiel R. New
609 insights of polyamine metabolism in testicular physiology: A role of ornithine decarboxylase
610 antizyme inhibitor 2 (AZIN2) in the modulation of testosterone levels and sperm motility.
611 PLoS One. 2018; 13(12): e0209202. doi: 10.1371/journal.pone.0209202
- 612 43. Seiler N. Liquid Chromatographic Methods for Assaying Polyamines Using
613 Prechromatographic Derivatization. Methods Enzymol. 1983; 94:10-2.
- 614 44. Tsirka S, Coffino P. Dominant negative mutants of ornithine decarboxylase. J Biol
615 Chem. 1992; 267: 23057-23062
- 616 45. Coleman CS, Stanley BA, Pegg AE. Effect of mutations at active site residues on the
617 activity of ornithine decarboxylase and its inhibition by active site-directed irreversible
618 inhibitors. J Biol Chem. 1993; 268: 24572-24579.
- 619 46. Tobias KE, Kahana C. Intersubunit Location of the Active Site of Mammalian
620 Ornithine Decarboxylase As Determined by Hybridization of Site-Directed Mutants.
621 Biochemistry. 1993; 32: 5842-5847.
- 622 47. Kidron H, Repo S, Johnson MS, Salminen TA. Functional classification of amino acid
623 decarboxylases from the alanine racemase structural family by phylogenetic studies. Mol Biol
624 Evol. 2007; 24: 79-89.
- 625 48. Ivanov IP, Firth AE, Atkins JF. Recurrent emergence of catalytically inactive ornithine
626 decarboxylase homologous forms that likely have regulatory function. J Mol Evol. 2010; 70(3):
627 289-302. doi: 10.1007/s00239-010-9331-5.

- 628 49. Pegg AE, McGill S. Decarboxylation of ornithine and lysine in rat tissues. BBA -
629 Enzymol. 1979; 568(2): 416-427.
- 630 50. Ghoda L, Van Daalen Wetters T, Macrae M, Ascherman D, Coffino P. Prevention of
631 rapid intracellular degradation of ODC by a carboxyl-terminal truncation. Science. 1989; 243:
632 1493-1495.
- 633 51. Rosenberg-Hasson Y, Bercovich Z, Kahana C. Characterization of sequences involved
634 in mediating degradation of ornithine decarboxylase in cells and in reticulocyte lysate. Eur J
635 Biochem. 1991; 196: 647-651.
- 636 52. Li X, Coffino P. Regulated degradation of ornithine decarboxylase requires interaction
637 with the polyamine-inducible protein antizyme. Mol Cell Biol. 1992; 12: 3556-3562 .
- 638 53. Hamana K, Matsuzaki S. Occurrence of sym-homospermidine in the Japanese newt,
639 *Cynops pyrrhogaster pyrrhogaster*. FEBS Lett. 1979; 99: 325-328.
- 640 54. Matsuzaki S, Tanaka S, Suzuki M, Hamana K. A possible role of cadaverine in the
641 biosynthesis of polyamines in the japanese newt testis. Endocrinol Jpn. 2011; 28 (3): 305-312.
- 642 55. Kurabuchi S, Matsuzaki S, Inoue S. Changes in polyamine content during limb
643 regeneration in adult *Xenopus laevis*. J Exp Zool. 1983; 227(1): 121-126.
- 644 56. López-Contreras AJ, Sánchez-Laorden BL, Ramos-Molina B, De La Morena ME,
645 Cremades A, Peñafiel R. Subcellular localization of antizyme inhibitor 2 in mammalian cells:
646 Influence of intrinsic sequences and interaction with antizymes. J Cell Biochem. 2009;
647 107(4):732-740. doi: 10.1002/jcb.22168.
- 648 57. Kanerva K, Mäkitie LT, Pelander A, Heiskala M, Andersson LC. Human ornithine
649 decarboxylase paralogue (ODCp) is an antizyme inhibitor but not an arginine decarboxylase.
650 Biochem J. 2007; 409(1): 187-192. doi: 10.1042/BJ20071004.

- 651 58. Kahana C. Protein degradation, the main hub in the regulation of cellular polyamines.
652 *Biochem J.* 2016; 473(24): 4551-4558. doi: 10.1042/BCJ20160519C
- 653 59. Ghoda L, Sidney D, Macrae M, Coffino P. Structural elements of ornithine
654 decarboxylase required for intracellular degradation and polyamine-dependent regulation. *Mol*
655 *Cell Biol.* 1992; 12: 2178-2185.
- 656 60. Li X, Coffino P. Degradation of Ornithine Decarboxylase: Exposure of the C-Terminal
657 Target by a Polyamine-Inducible Inhibitory Protein Downloaded from. *Mol Cell Biol.* 1993;
658 13: 2377–2383.
- 659 61. Zhang M, Pickart CM, Coffino P. Determinants of proteasome recognition of ornithine
660 decarboxylase, a ubiquitin-independent substrate. *EMBO J.* 2003; 22: 1488-1496.
- 661 62. Prakash S, Tian L, Ratliff KS, Lehotzky RE, Matouschek A. An unstructured initiation
662 site is required for efficient proteasome-mediated degradation. *Nat Struct Mol Biol.* 2004; 11:
663 830–837.
- 664 63. Berko D, Tabachnick-Cherny S, Shental-Bechor D, Cascio P, Mioletti S, Levy Y, et al.
665 The Direction of Protein Entry into the Proteasome Determines the Variety of Products and
666 Depends on the Force Needed to Unfold Its Two Termini. *Mol Cell.* 2012; 48(4): 601-611. doi:
667 10.1016/j.molcel.2012.08.029.
- 668
- 669
- 670
- 671
- 672

673 **Supporting information**

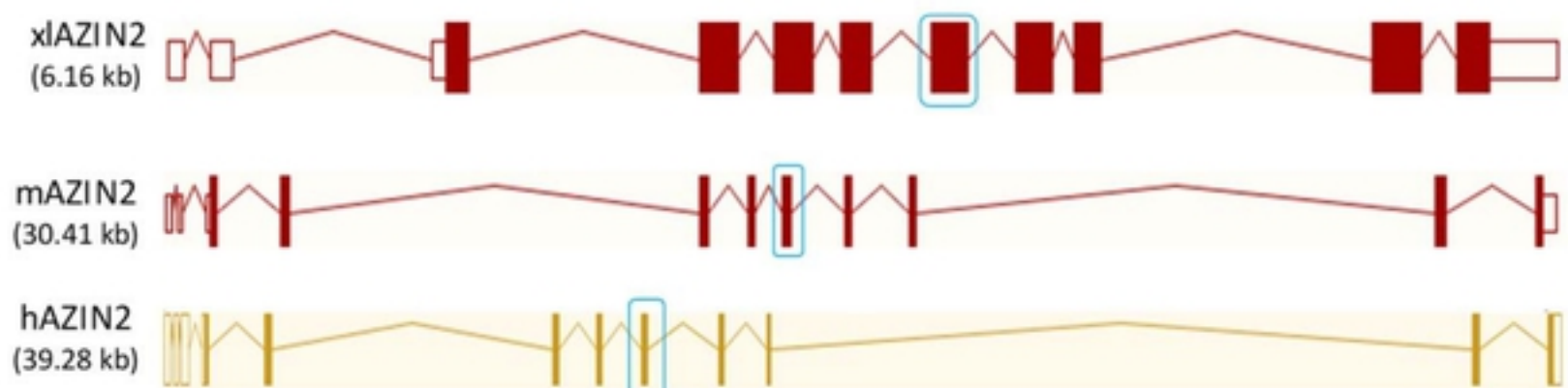
674 **S1 Fig. Comparison of the amino acid sequences of *Xenopus laevis* AZIN2 (xlAZIN2) and**
675 ***Xenopus tropicalis* AZIN2 (xtAZIN2) using ClustalW program for multiple sequence**
676 **alignment.** Asterisks represent amino acid identity; colon and dots represent amino acid
677 similarity between the proteins. Grey background indicates amino acid residues associated with
678 the catalytic activity of mODC that are conserved in the *Xenopus* homologues.

679 **S2 Fig. Sequences of the C-terminal region of mODC and its paralogues and *Xenopus***
680 ***laevis* orthologue proteins.** (A) Scheme of the C-terminal region of mODC, where C represent
681 the ~70 amino acid residues, and S1 and S2 the two subregions that may be important for
682 proteasomal degradation of ODC induced by AZ1. (B) Detailed sequence of the C-terminal
683 region of mODC and its different paralogues and orthologues. Sequences corresponding to S1
684 (residues 391-420) and S2 (residues 441-461) are underlined.

685 **S3 Fig. Influence of AZ1 on protein levels of xlAZIN1.** HEK293T cells were transfected
686 with xlAZIN1-Flag alone or in combination with AZ1. Western-blot were probed with anti-
687 Flag and anti-ERK2 antibodies.

688 **S1 Table. Sequence identity between the C-terminal region of mODC and those of its**
689 ***Xenopus laevis* homologues.** C: terminal region from residues 391 to 461 in mODC; S1 and
690 S2 are two subregions that may be important for ODC proteasomal degradation induced by
691 AZ1; S1: residues 391-423; S2: residues 441-461. (See S2 Fig).

692



bioRxiv preprint doi: <https://doi.org/10.1101/661843>; this version posted June 5, 2019. The copyright holder for this preprint (which was not certified by peer review) is the author/funder, who has granted bioRxiv a license to display the preprint in perpetuity. It is made available under aCC-BY 4.0 International license.

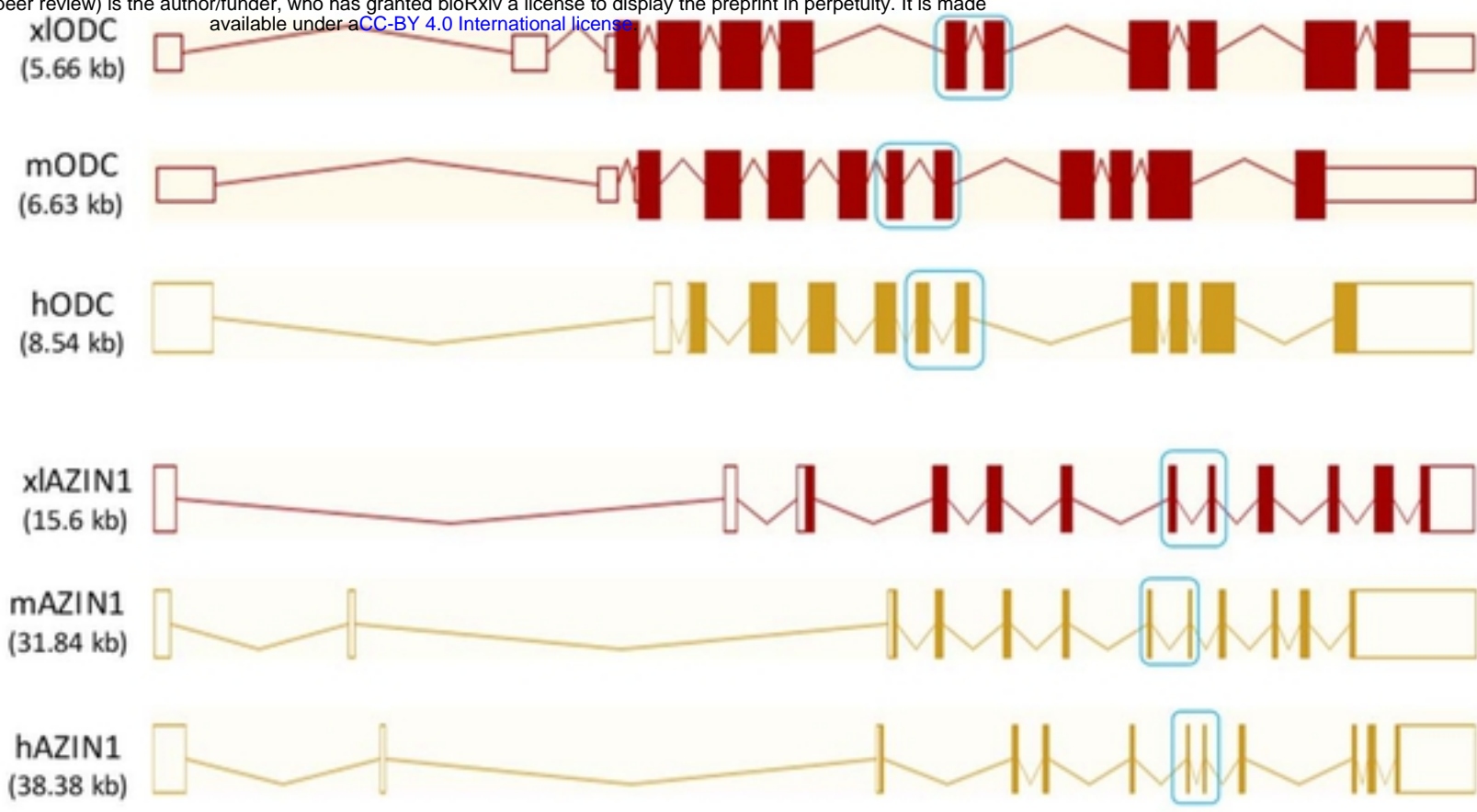


Figure 1

bioRxiv preprint doi: <https://doi.org/10.1101/661843>; this version posted June 5, 2019. The copyright holder for this preprint (which was not certified by peer review) is the author/funder, who has granted bioRxiv a license to display the preprint in perpetuity. It is made available under aCC-BY 4.0 International license.

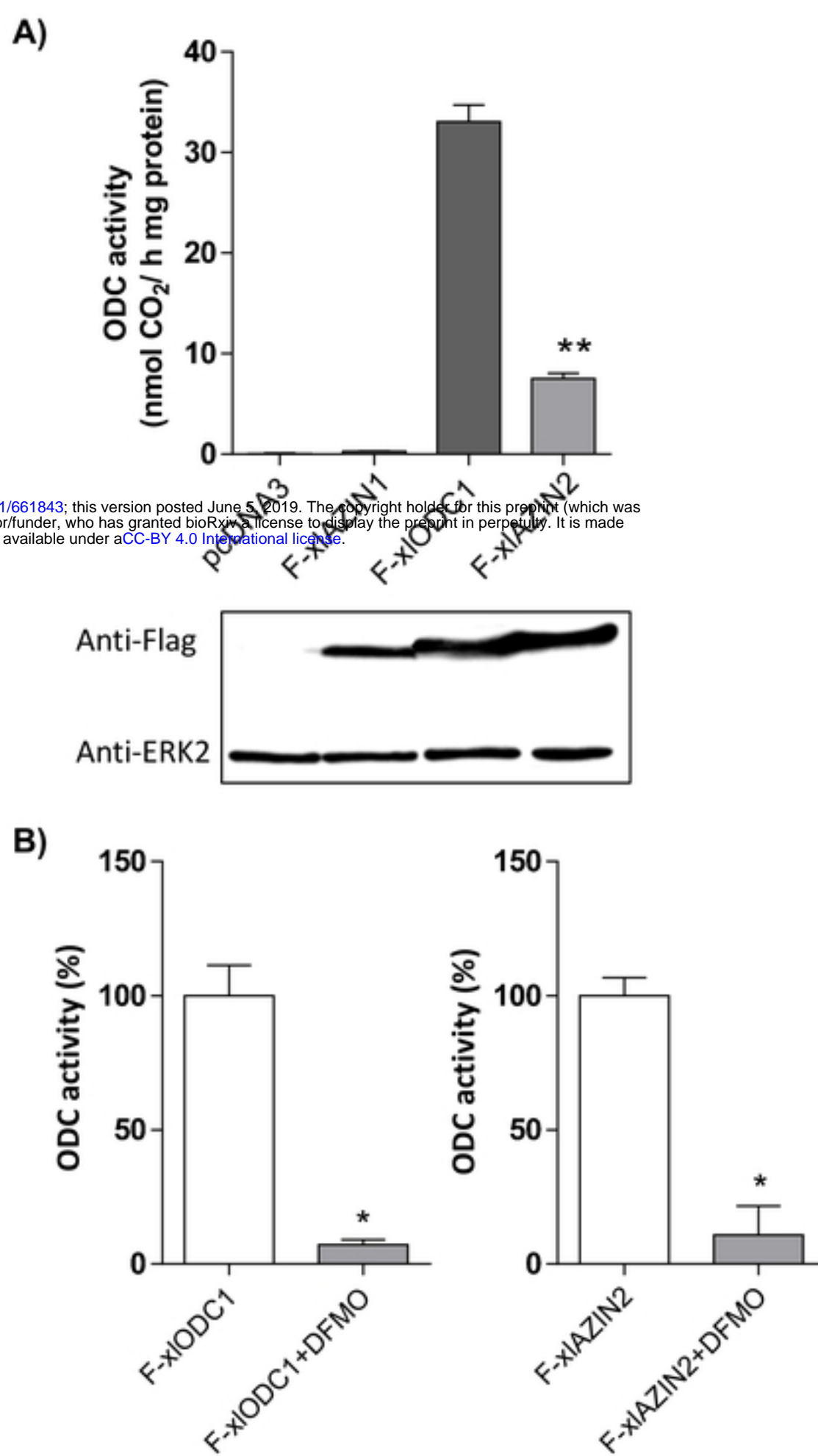


Figure 3

bioRxiv preprint doi: <https://doi.org/10.1101/661843>; this version posted June 5, 2019. The copyright holder for this preprint (which was not certified by peer review) is the author/funder, who has granted bioRxiv a license to display the preprint in perpetuity. It is made available under aCC-BY 4.0 International license.

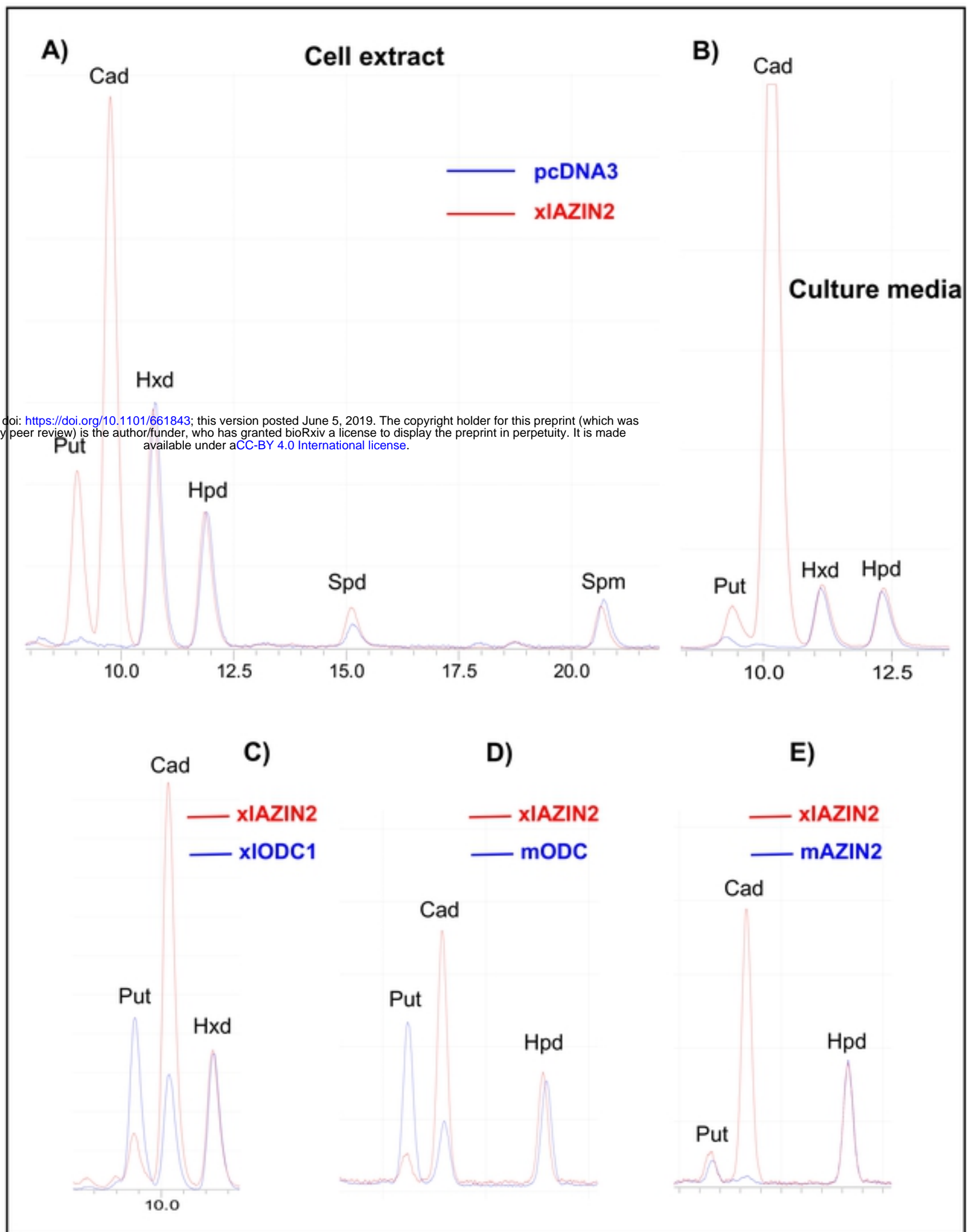


Figure 4

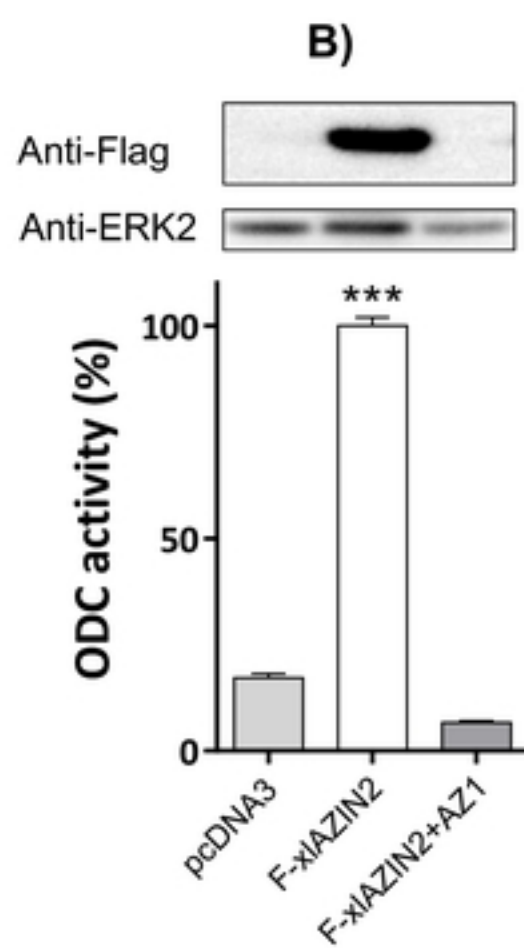
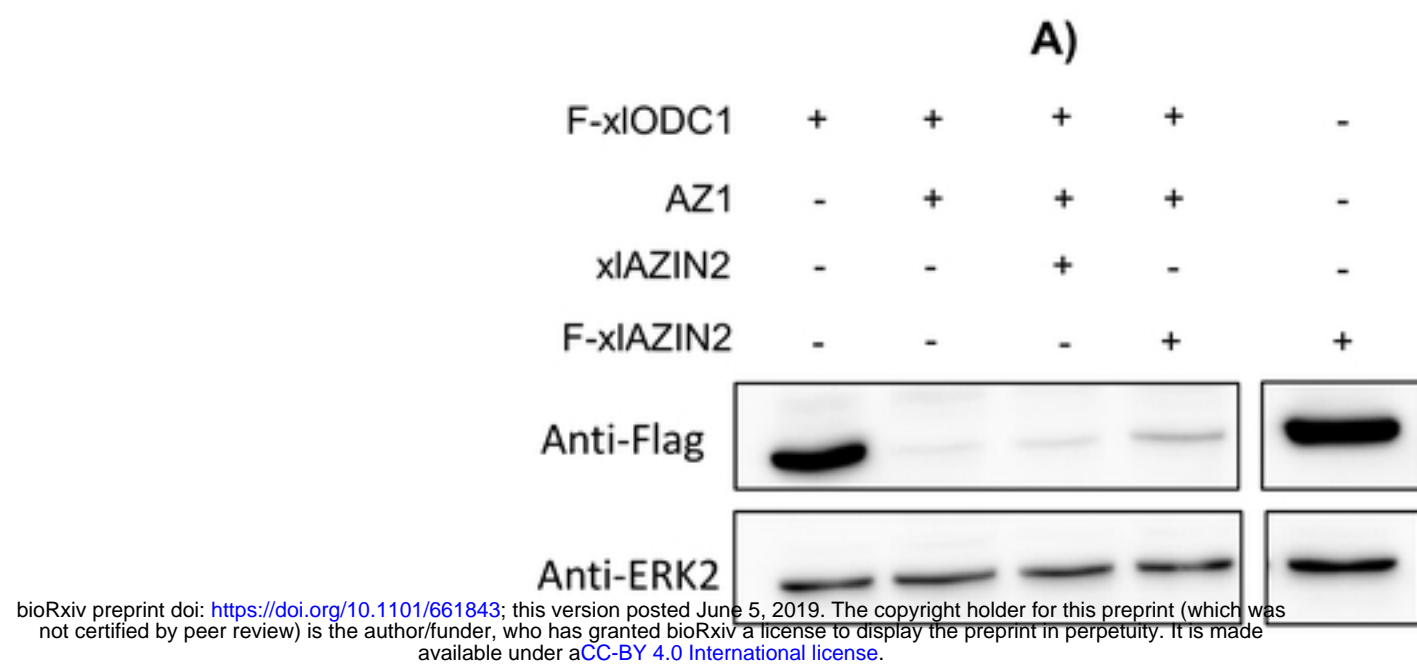


Figure 5

bioRxiv preprint doi: <https://doi.org/10.1101/661843>; this version posted August 19, 2019. The copyright holder for this preprint (which was not certified by peer review) is the author/funder, who has granted bioRxiv a license to display the preprint in perpetuity. It is made available under aCC-BY 4.0 International license.

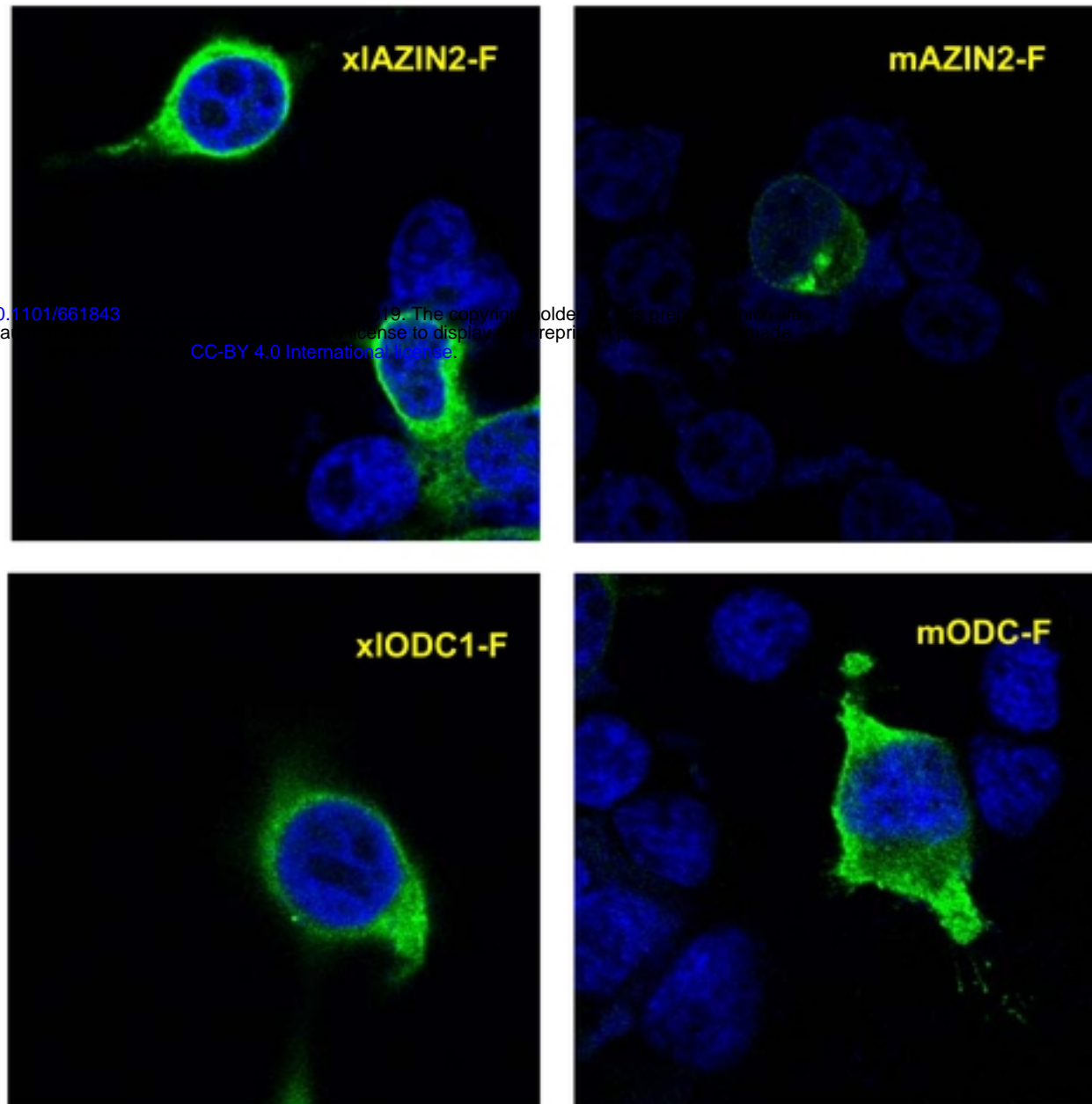


Figure 6

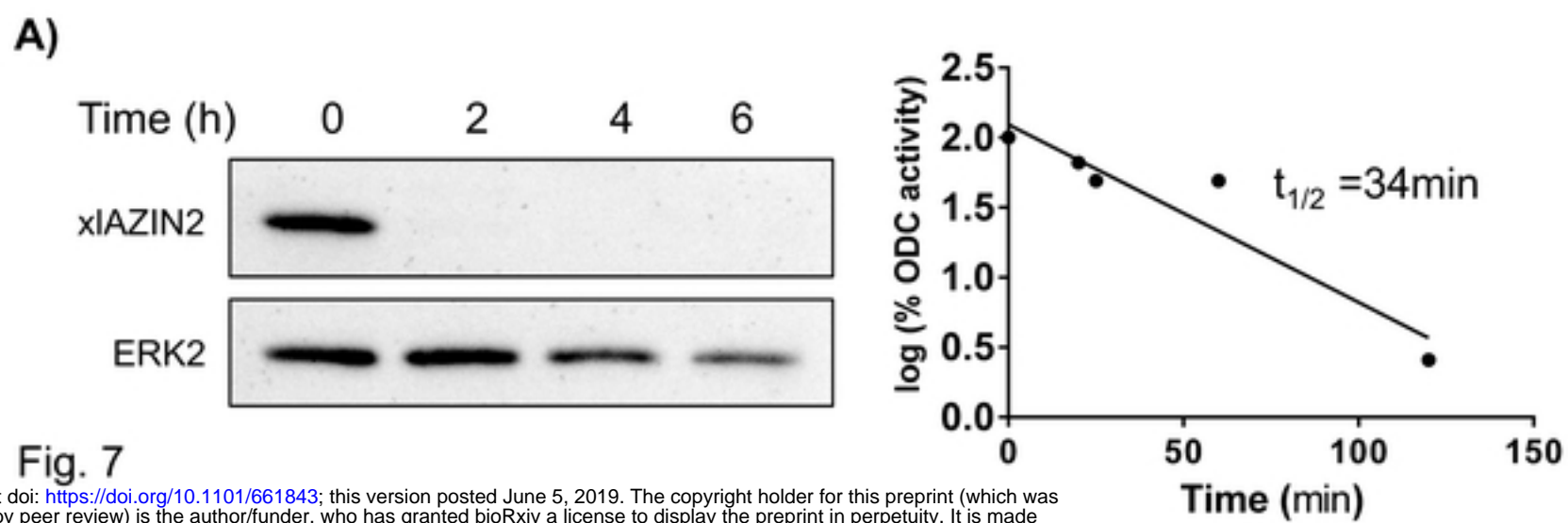
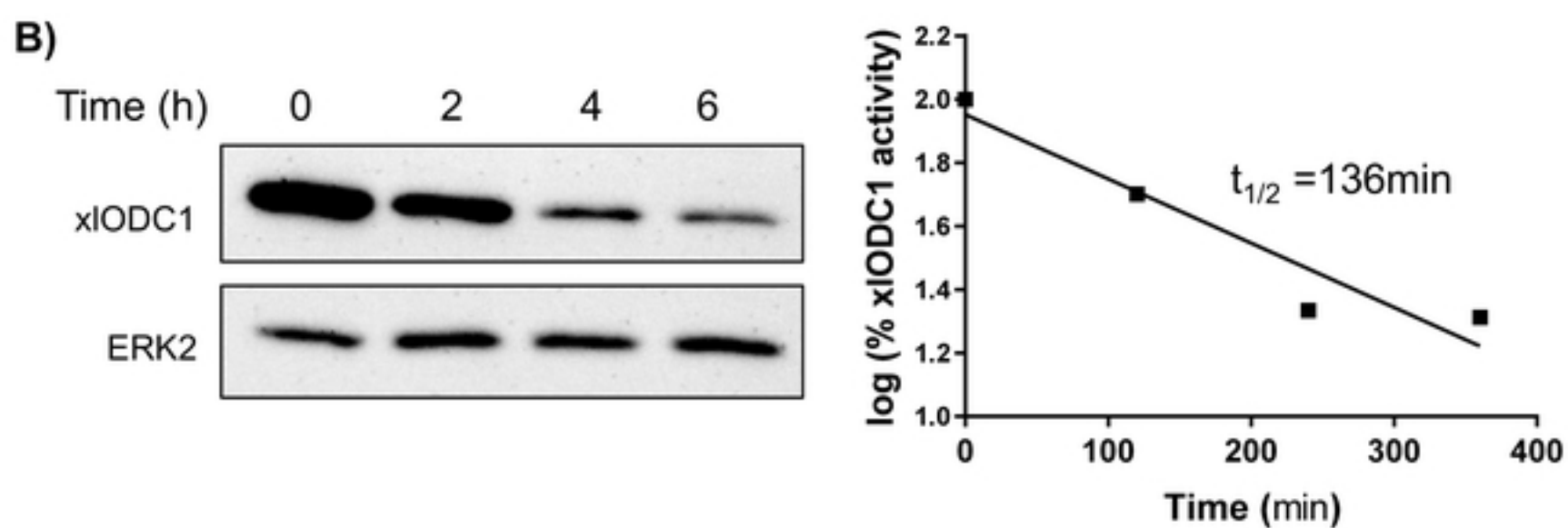
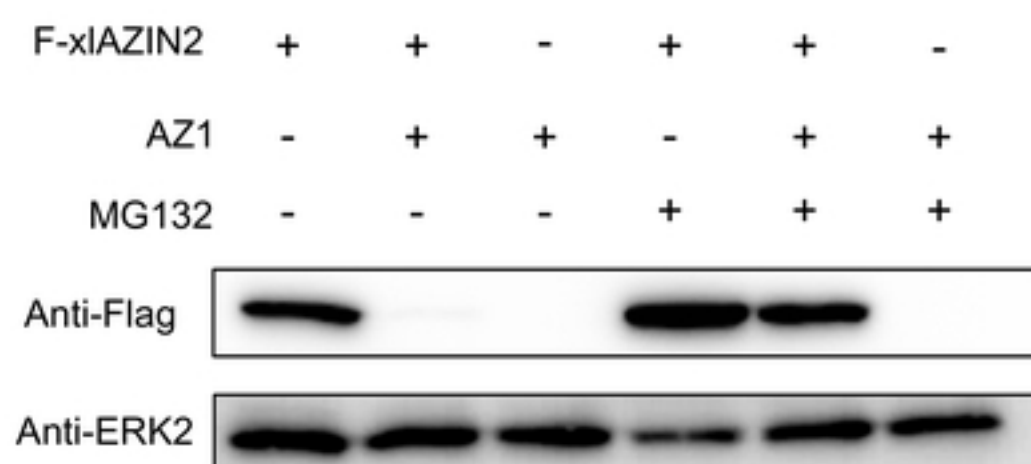


Fig. 7

bioRxiv preprint doi: <https://doi.org/10.1101/661843>; this version posted June 5, 2019. The copyright holder for this preprint (which was not certified by peer review) is the author/funder, who has granted bioRxiv a license to display the preprint in perpetuity. It is made available under aCC-BY 4.0 International license.



C)



bioRxiv preprint doi: <https://doi.org/10.1101/041244>; this version posted June 5, 2019. The copyright holder for this preprint (which was not certified by peer review) is the author/funder, who has granted bioRxiv a license to display the preprint in perpetuity. It is made available under aCC-BY 4.0 International license.

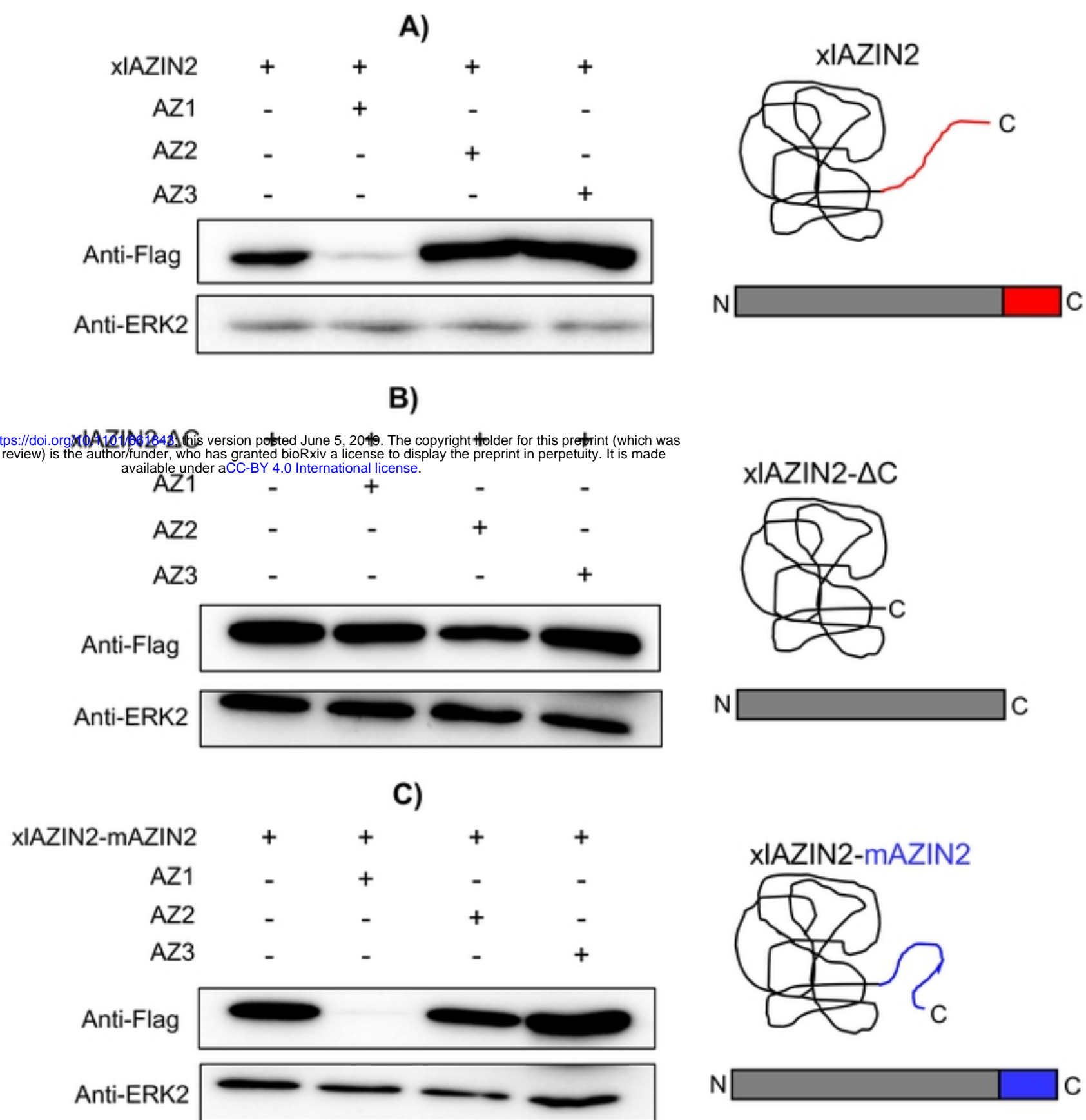
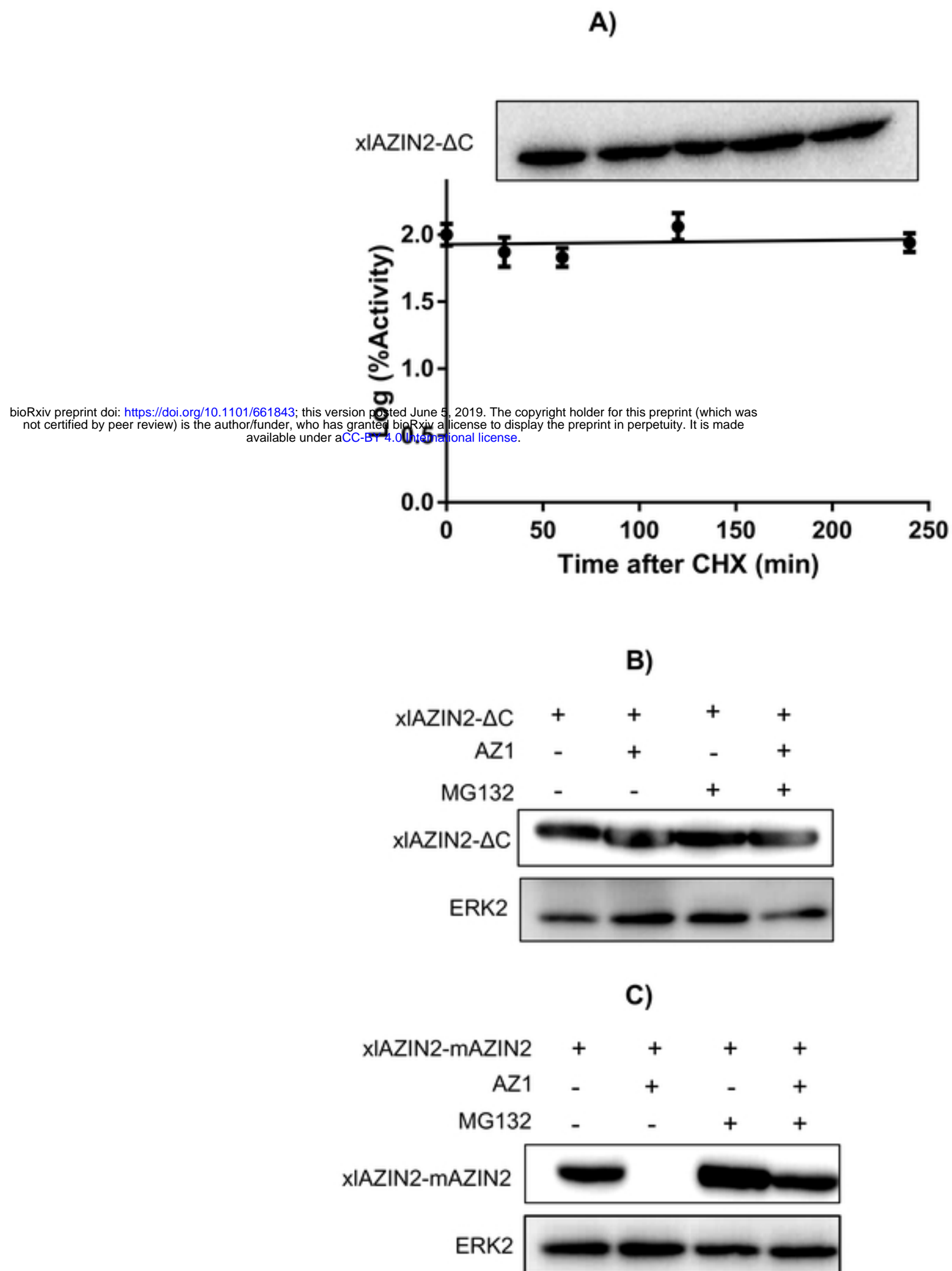


Figure 8



bioRxiv preprint doi: <https://doi.org/10.1101/661843>; this version posted June 5, 2019. The copyright holder for this preprint (which was not certified by peer review) is the author/funder, who has granted bioRxiv a license to display the preprint in perpetuity. It is made available under aCC-BY 4.0 International license.